ADVANCED FUNCTIONAL MATERIALS

Supporting Information

for *Adv. Funct. Mater.*, DOI: 10.1002/adfm.201906189

Intrinsic Lithiophilicity of Li–Garnet Electrolytes Enabling High-Rate Lithium Cycling

Hongpeng Zheng, Shaoping Wu, Ran Tian, Zhenming Xu, Hong Zhu, Huanan Duan, and Hezhou Liu*

Supporting Information

Intrinsic lithiophilicity of Li-garnet-electrolytes enabling high-rate lithium cycling

Hongpeng Zheng[1], Shaoping Wu[1], Ran Tian[1], Zhenming Xu[2], Hong Zhu[2], Huanan Duan[1], Hezhou Liu[1]*

1 State Key Laboratory of Metal Matrix Composites, School of Materials Science and Engineering, Shanghai Jiao Tong University, Shanghai 200240, P. R. China
2 University of Michigan-Shanghai Jiao Tong University Joint Institute, Shanghai Jiao Tong University, Shanghai 200240, China

Methods

Materials synthesis. All the reagents—unless otherwise noted—were purchased from Sinopharm Chemical Reagent Co., Ltd. The garnet pellets used in this study was synthesized via conventional solid-state reaction reported previously.[1] Briefly, proper amount of Li_2CO_3 (99.99 %, with 10% excess to compensate the sintering loss), La_2O_3 (99.95 %), ZrO_2 (99.97 %), Ta_2O_5 (99.99 %) were ground in a mortar to obtain stoichiometry of $Li_{6.4}La_3Zr_{1.4}Ta_{0.6}O_{12}$ (designated as LLZT). The mixture was calcined at 900 °C for 6 h, then the obtained mother powders were reground and pressed into pellets with a diameter of 10 mm before sintering at 1140 °C for 16 h. The resulting LLZT pellets are 1 mm thick with a surface area of 1.13 cm^2. The pellets were polished with P2000 sand paper and stored in an Ar-filled glovebox (<0.1 ppm O_2, <0.1 ppm H_2O) to prevent reactions with air. Some LLZT pellets were

intentionally stored in humid air for 1 week to form a thin-layer Li_2CO_3 on the surface as previously reported.[15b]

Computational methods and models. All calculations were carried out by using the projector augmented wave method in the framework of the density functional theory,[3] as implemented in the Vienna *ab*-initio Simulation Package (VASP). The generalized gradient approximation (GGA) and Perdew–Burke–Ernzerhof (PBE) exchange functional[3] was used. Structural relaxation calculations were performed by using the spin-polarized GGA method.[4] The plane-wave energy cutoff was set to 500 eV. The Monkhorst–Pack method[5] with 1×1×1, 1×1×1, 7×7×7, 5×5×5 and 3×3×2 *k*-meshes were employed for the Brillouin zone sampling of $Li_7La_3Zr_2O_{12}$,$Li_{6.4}La_3Zr_{1.4}Ta_{0.6}O_{12}$, Li, Li_2O and Li_2CO_3 bulks, respectively. For the interface calculations with large supercells, we just need to use the 1×1×1 *k*-mesh. The convergence criterions of energy and force calculations were set to 10^{-5} eV/atom and 0.01 eV $Å^{-1}$, respectively. The $Li_7La_3Zr_2O_{12}$ (001)/Li (001), $Li_{6.4}La_3Zr_{1.4}Ta_{0.6}O_{12}$ (001)/Li (001), Li_2CO_3 (001) /Li (001) and Li_2O (001) /Li (001) interface models were constructed by $Li_7La_3Zr_2O_{12}$ (001) slab, $Li_{6.4}La_3Zr_{1.4}Ta_{0.6}O_{12}$ (001) slab, Li_2CO_3 (001) slab, Li_2O (001) slab and Li(001) slab, which are the low-energy surfaces.[6] The coherent interface approximation was applied, in which the soft Li(001) 4×4 surface slabs are less strained to match the dimensions of the pristine and Ta doped-$Li_7La_3Zr_2O_{12}$ (001)1×1,and Li_2O (001)3×3 surface slabs. The Li(001) 3×2 surface slab is less strained to match the Li_2CO_3 (001) 2×2 surface slab.

To evaluate the wettability of Li metal on the $Li_7La_3Zr_2O_{12}$, $Li_{6.4}La_3Zr_{1.4}Ta_{0.6}O_{12}$, Li_2O and Li_2CO_3 surfaces, we calculated the interface formation energies of $Li_7La_3Zr_2O_{12}$ (001)/Li (001), $Li_{6.4}La_3Zr_{1.4}Ta_{0.6}O_{12}$ (001)/Li (001), Li_2CO_3 (001) /Li (001) and Li_2O (001)/Li (001) systems, which can be evaluated by energy difference between an interface system and the bulk energy of the two materials that comprise it, $E_f = (E_{ab} - N_a*E_a - N_b*E_b)/2S$,[7] here, E_{ab} denotes the total energy of the complete system containing the interface, and it depends on how many formula units of materials *a* and *b* comprise the interface (*Na* and *Nb*, respectively). E_a and E_b denote the bulk energy per formula unit for materials *a* and *b*, respectively, and S refers to the interfacial area, 2 means two interfaces in the interface models.

Physicochemical Characterization. Scanning electron microscopy (SEM) images were taken on a TESCAN Mira3 field emission scanning electron microscope (FESEM). Time-of-flight secondary ion mass spectrometry (TOF-SIMS) and TOF-SEM were carried out on a TESCAN Gaia3 FESEM. ATOF-SIMS 5-100 instrument (ION TOF) was attached to the TESCAN GAIA3 FESEM. The samples were pre-beamed to wipe off the influence of air exposure. Raman spectra were recorded on a DXR Raman microscope (Senterra R200-L) with an excitation length of 532 nm. The structural characterization was performed by X-ray diffraction (XRD, D/MAX255ovl/84, Rigaku, Japan) with 2θ in the range of 10 ~ 60^o with a step size of 0.02^o. The ionic conductivity was calculated from data collected by an impedance analyzer (Solartron 1260) in the frequency range from 10 MHz to 1 Hz with a 10 mV amplitude.

Battery assembly and electrochemical tests. A symmetric cell was assembled in an Ar-filled glovebox by two methods: 1) stacking lithium garnets between two Li foils (Aladdin, 200 μm thick, designated as Li_s/LLZT/Li_s) and heating up to 300 ^oC to improve the Li/LLZT contact; and 2) rubbing lithium garnets on molten Li till the Li wets the garnet surface (designated as Li_r/LLZT/Li_r, as shown in Video S1), followed by cooling down and coin-cell making. The resistance values of garnet/Li interface were calculated based on dividing experimental resistance by two, and then normalizing to the contact interface area. The lithium plating/stripping test was carried out by galvanostatic cycling with a LAND CT2001A cell test system at various current densities at room temperature and 60 °C. In cylic voltammetry tests, an LLZT pellet was sandwiched between stainless steel sheet as the working electrode, and Li foil as the reference and counter electrode with a scan rates of 1 mVs^{-1} from -0.1 V to 6 V in a coin cell. Morphology study was performed before and after cycling tests using a scanning electron microscopy (SEM, TM 3000 tabletop microscope, Hitachi) equipped with Energy-dispersive X-ray spectra (EDS).

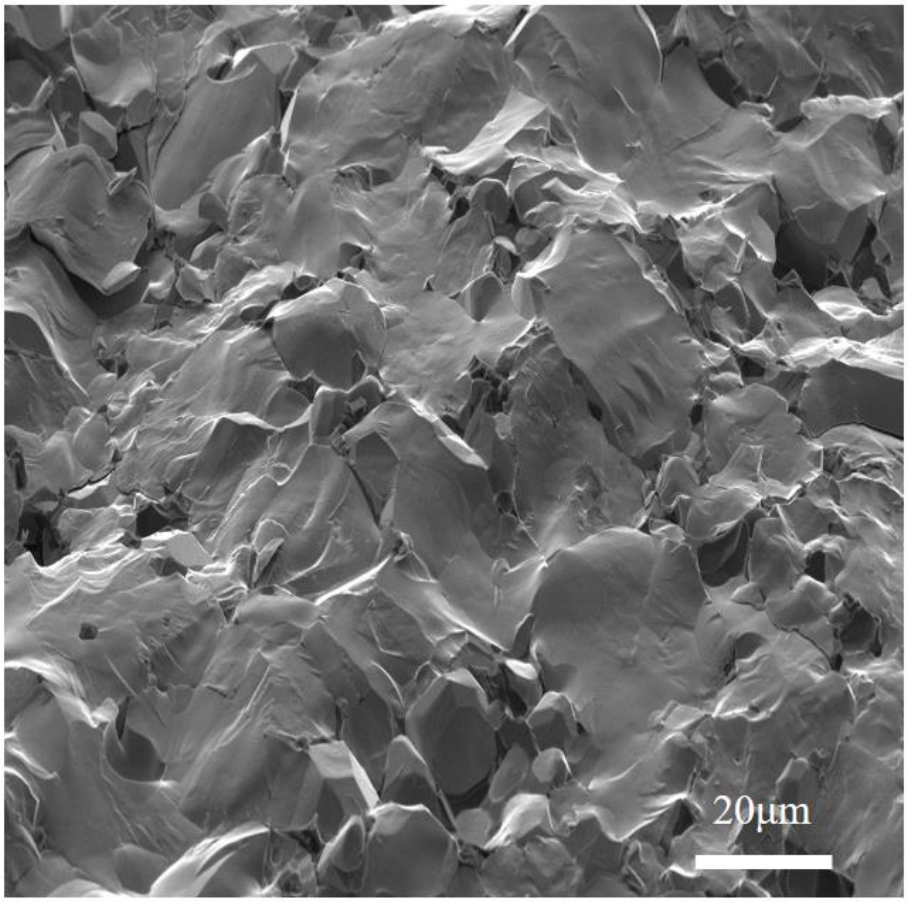

Fig. S1 SEM image of the LLZT pellets.

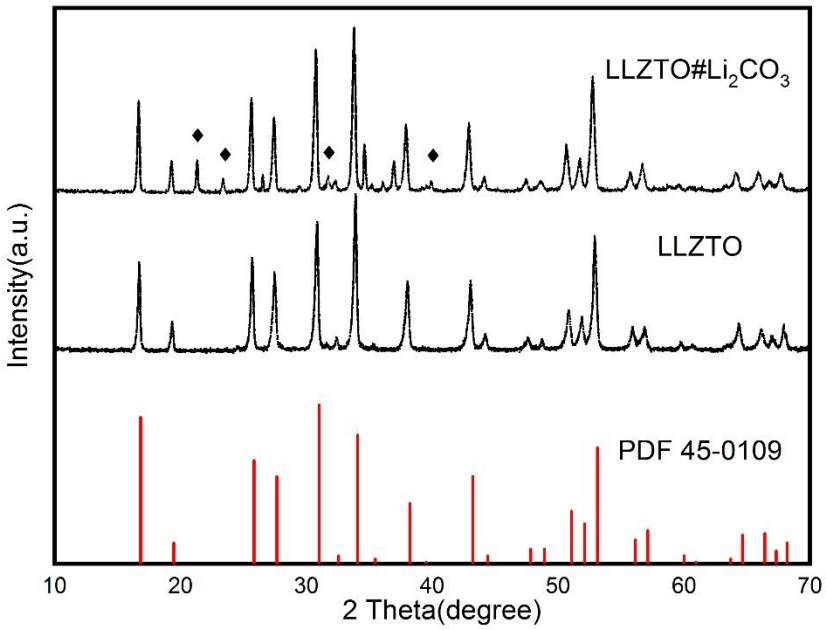

Fig. S2 XRD patterns of the LLZT pellets with and without the Li_2CO_3 surface layer.

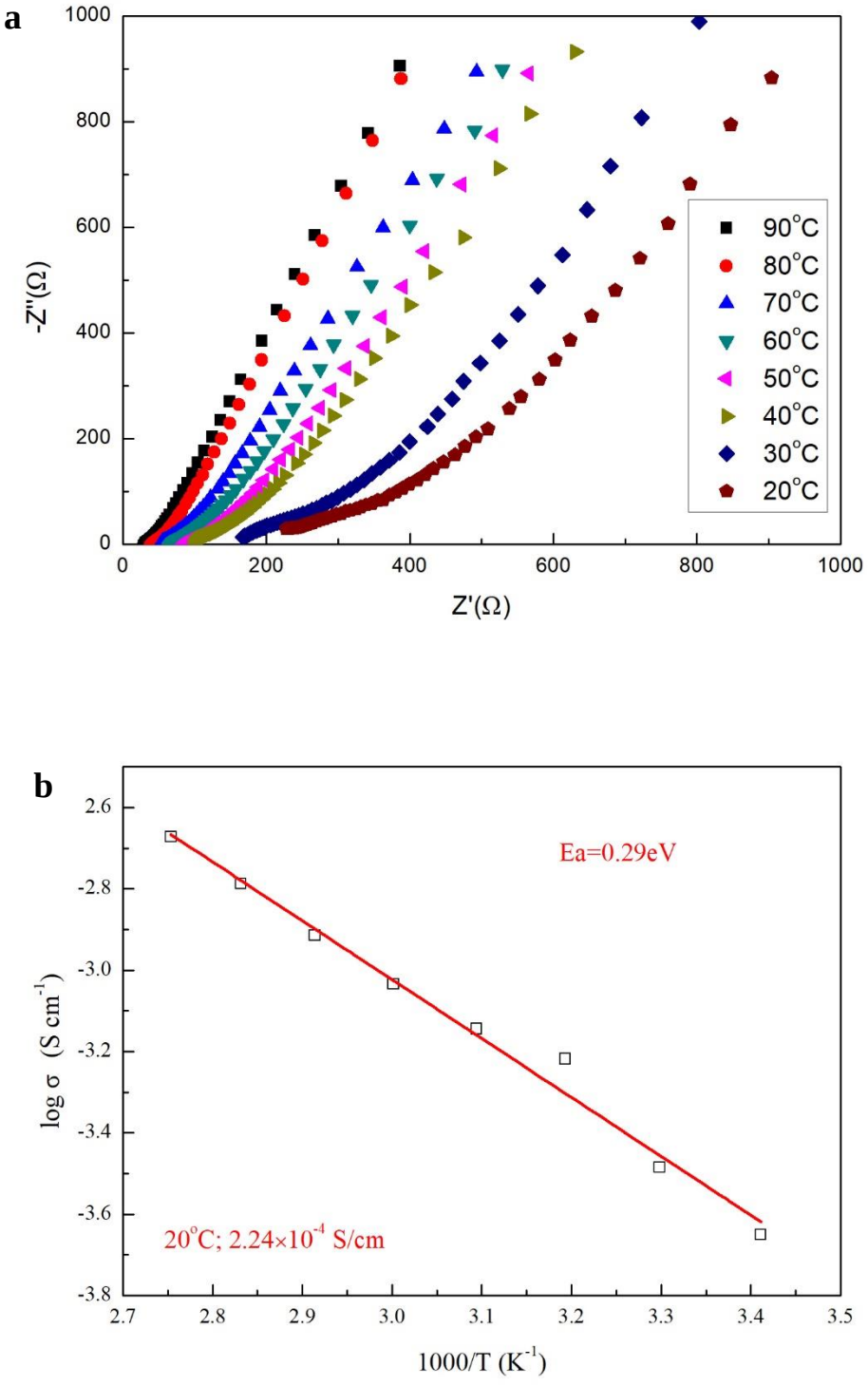

Fig. S3 (a) EIS of the LLZT pellets with blocking Ag electrodes at different temperatures. (b) Arrhenius plot of the LLZT ionic conductivity.

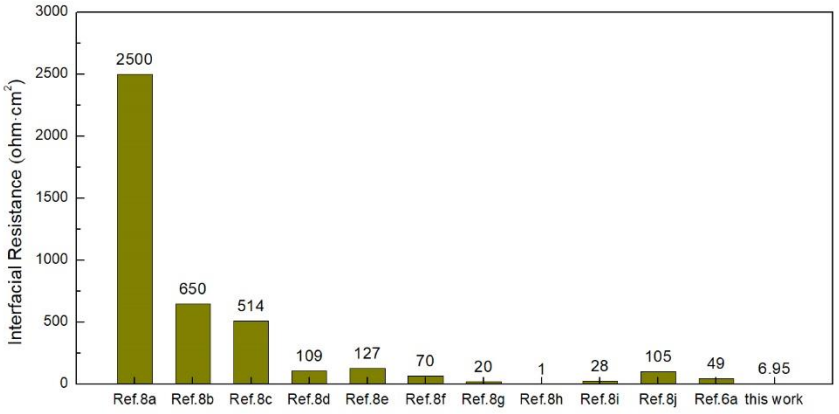

Fig. S4 A comparison of the Li/garnet interface resistances from representative works and ours.[6a, 8]

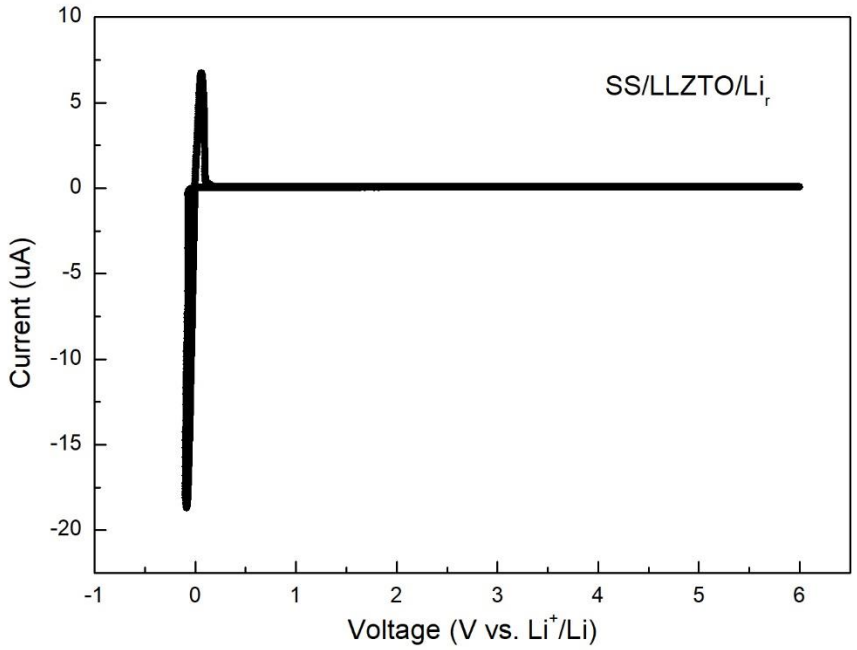

Fig. S5 CV curve of LLZT with stainless steel (SS) as working electrode and Li_r as reference electrode. The voltage scan rate is 1 mV s^{-1}.

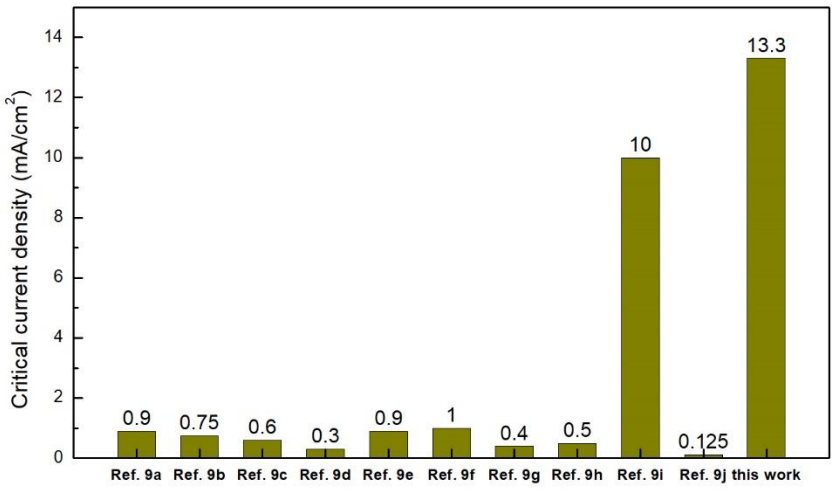

Fig. S6 A comparison of the critical current densities at room temperature from representative works and ours.[9]

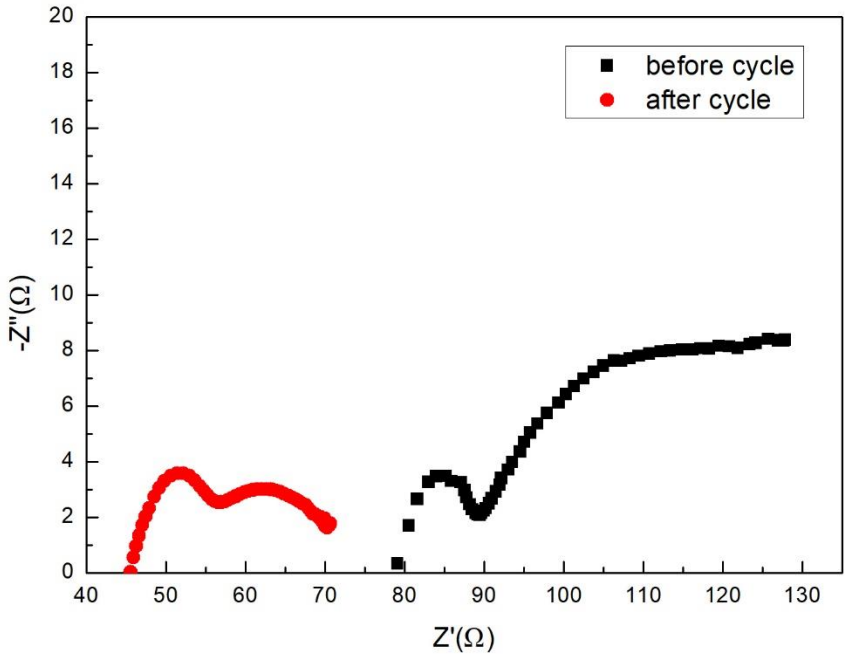

Fig. S7 Nyquist plots of the Li_r/LLZT/Li_r cells before and after cycling tests at a current density of ±13.3 mA cm^{-2} with a capacity of 0.4 mAh cm^{-2} at room temperature for 500 cycles.

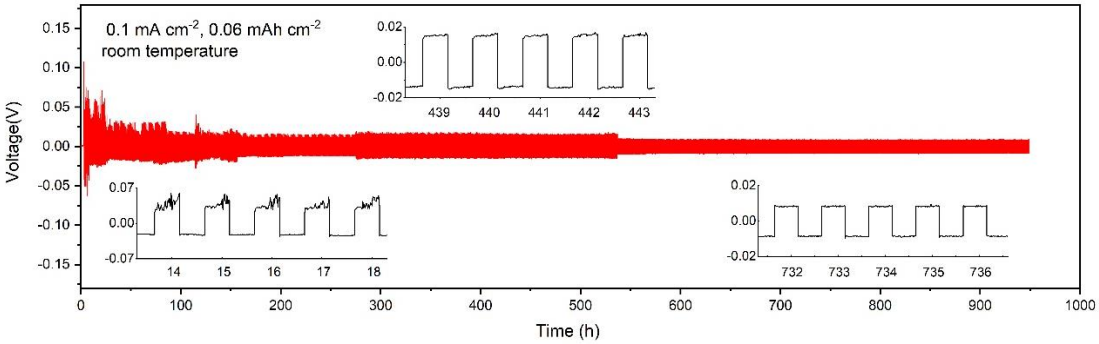

Fig. S8 Galvanostatic cycling of Li_r/LLZT/Li_r at ±0.1 mA cm^{-2} with a capacity of 0.06 mAh cm^{-2} for 950 hours.

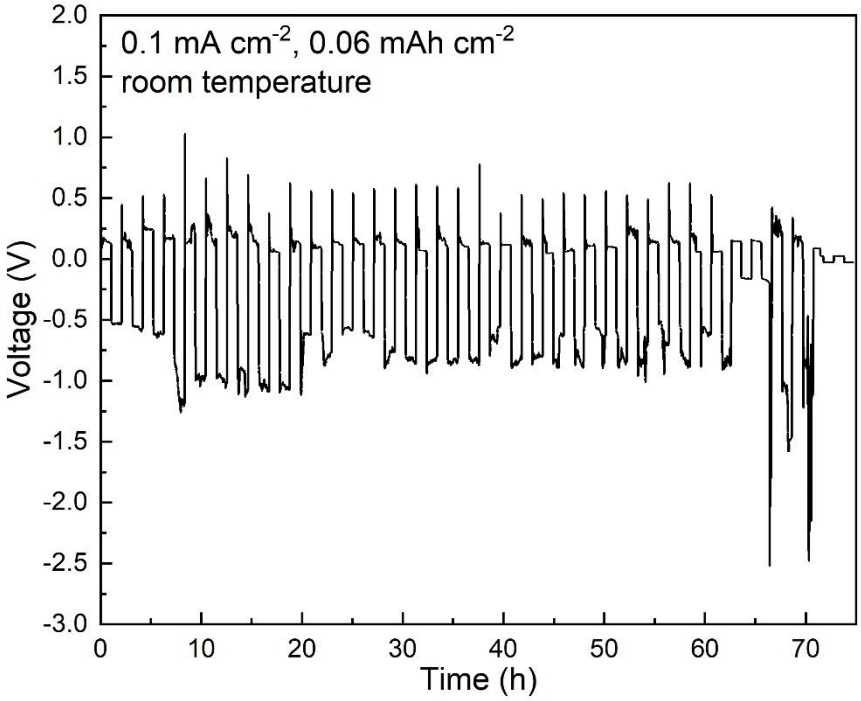

Fig. S9. Galvanostatic cycling of Li_s/LLZT/Li_s at room temperature and at ±0.1 mA cm^{-2} with a capacity of 0.05 mAh cm^{-2} for 75 hours.

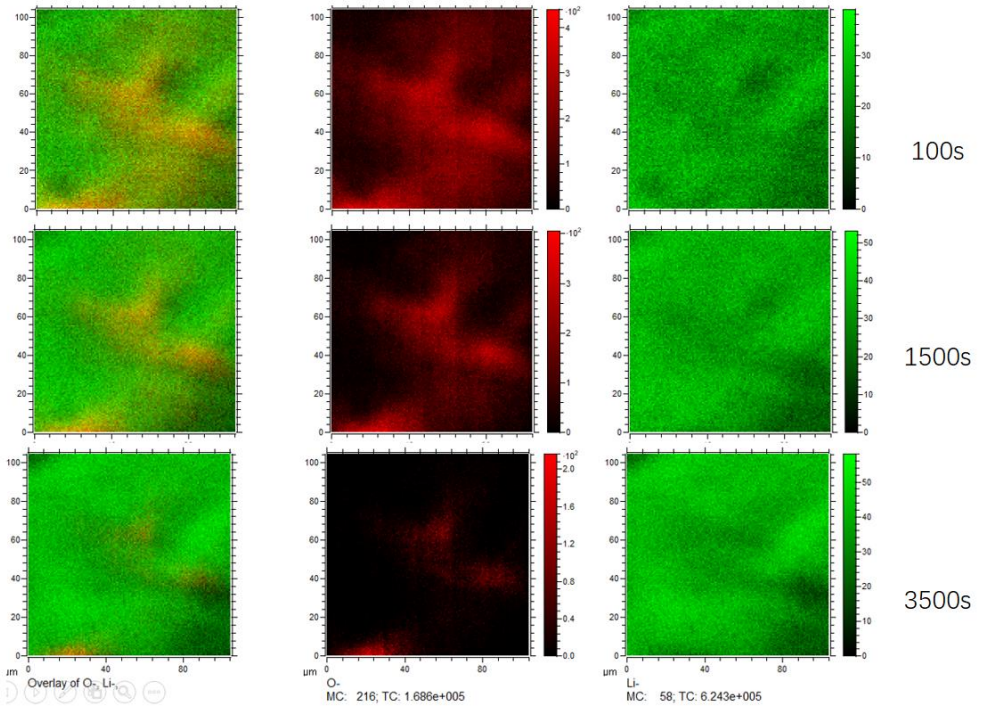

Fig. S10 TOF-SIMS characterization of Li metal. High-resolution maps (100 × 100 μm^2) of the O and Li secondary ion (SI) signals after shallow (100 s) and heavy (3500 s) sputtering.

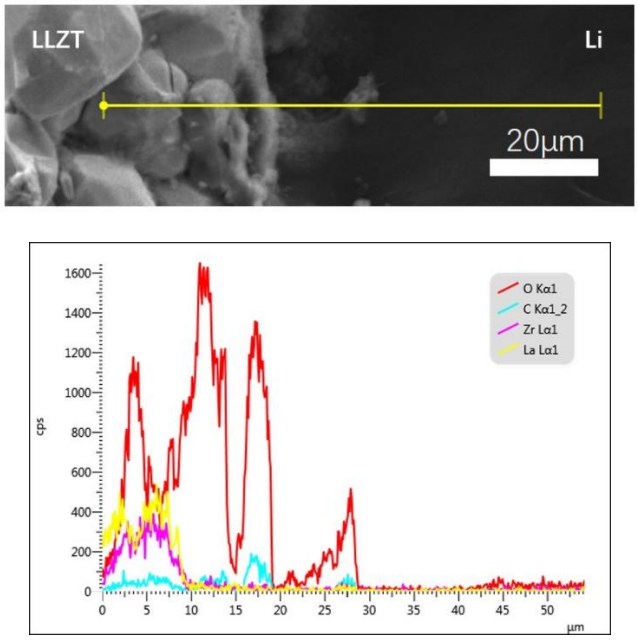

Fig. S11 SEM photograph (a) and EDS line scan (b) of the Li/LLZT (with Li_2CO_3) interface.

Fig. S12 Digital photos of the melted Li metal on top of the pure Li_2CO_3 pellets after rub-coating molten Li.

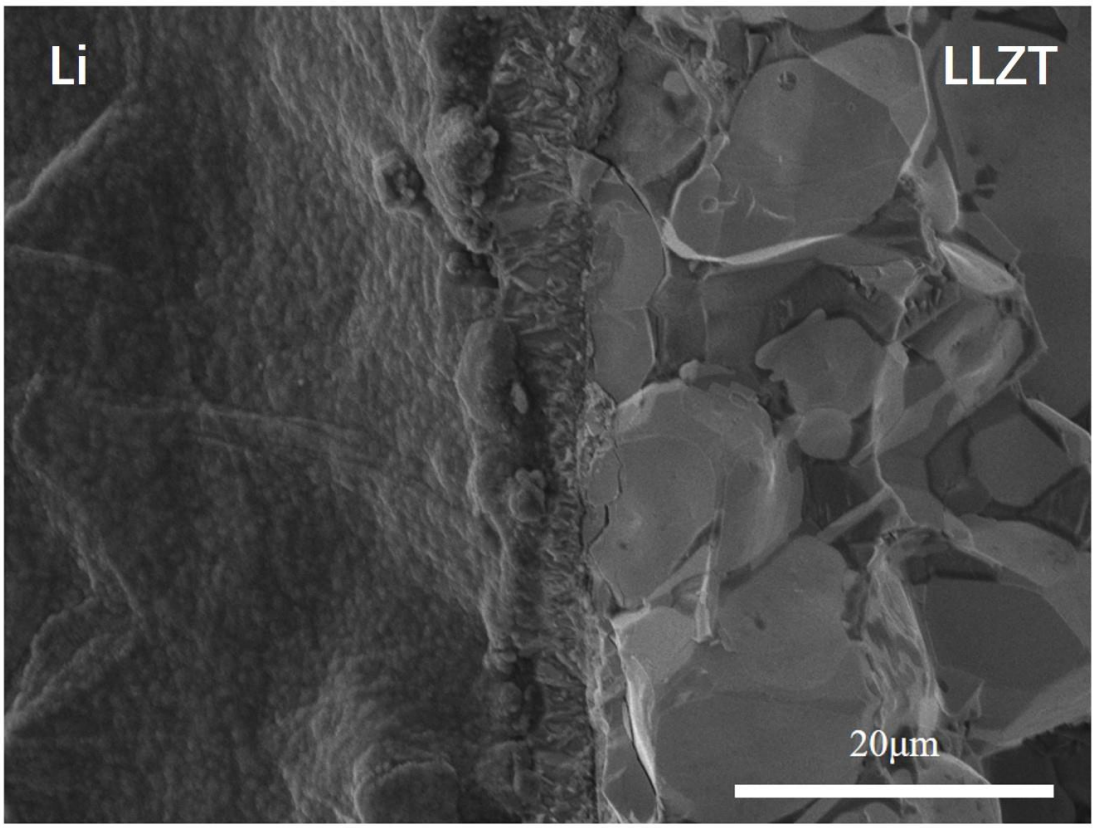

Fig. S13 SEM images of the Li/LLZT (with Li_2CO_3) interface after rub-coating molten Li.

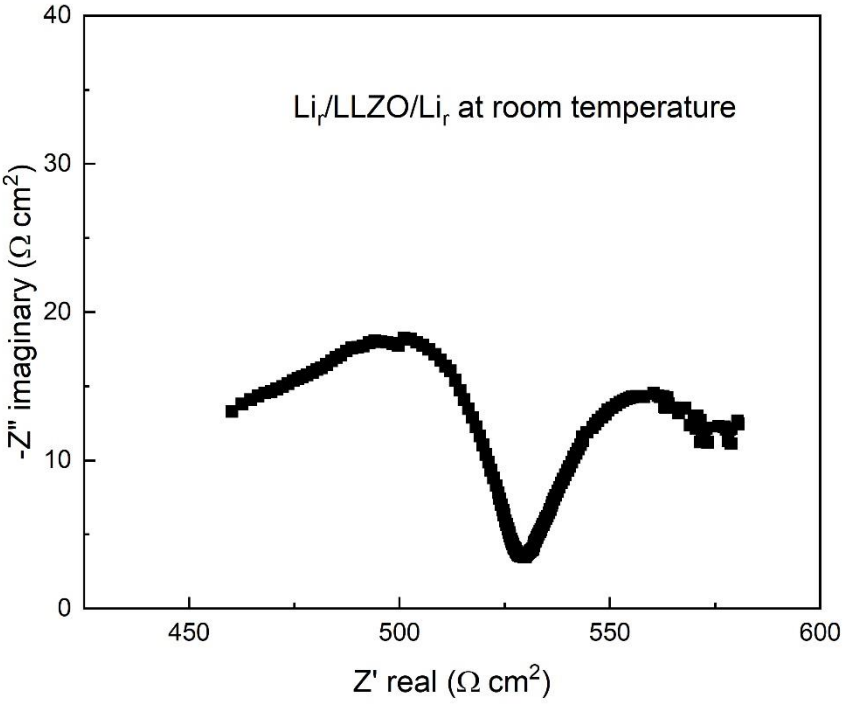

Fig. S14 Nyquist plots of the Li_r/LLZO/Li_r symmetric cells at room temperature.

Supplementary Table 1 | The interface formation energies (in J/m^2) of $Li_7La_3Zr_2O_{12}$ (001)/Li (001), $Li_{6.4}La_3Zr_{1.4}Ta_{0.6}O_{12}$ (001)/Li (001), Li_2CO_3 (001) /Li (001) and Li_2O (001)/Li (001) systems.

	$Li_7La_3Zr_2O_{12}$ (001)/Li (001)	$Li_{6.4}La_3Zr_{1.4}Ta_{0.6}O_{12}$ (001)/Li (001)	Li_2CO_3 (001) /Li (001)	Li_2O (001)/Li (001)
E_f (in J/m^2)	-2.52	-6.14	-0.63	0.23

Supplementary References:

[1] B. Xu, H. Duan, W. Xia, Y. Guo, H. Kang, H. Li, H. Liu, *J. Power Sources* **2016**, 302, 291.

[2] W. Xia, B. Xu, H. Duan, Y. Guo, H. Kang, H. Li, H. Liu, *ACS Appl. Mater. Interfaces* **2016**, 8, 5335.

[3] W. Kohn, L. J. Sham, *Phys. Rev. B* **1965**, 140, A1133.

[4] S. L. Dudarev, G. A. Botton, S. Y. Savrasov, C. J. Humphreys, A. P. Sutton, *Phys. Rev. B* **1998**, 57, 1505.

[5] H. J. Monkhorst, J. D. Pack, *Phys. Rev. B:* **1976**, 13, 5188.

[6] a) J.-F. Wu, B.-W. Pu, D. Wang, S.-Q. Shi, N. Zhao, X. Guo, X. Guo, *ACS Appl. Mater. Interfaces* **2019**, 11, 898; b) M. Bruno, M. Prencipe, *Surf. Sci.* **2007**, 601, 3012; c) L. Pastero, F. R. Massaro, D. Aquilano, *Cryst. Growth Des.* **2007**, 7, 2749.

[7] N. D. Lepley, N. A. W. Holzwarth, *Phys. Rev. B:* **2015**, 92, 214201.

[8] a) H. Buschmann, J. Dölle, S. Berendts, A. Kuhn, P. Bottke, M. Wilkening, P. Heitjans, A. Senyshyn, H. Ehrenberg, A. Lotnyk, V. Duppel, L. Kienle, J. Janek, *Phys. Chem. Chem. Phys.* **2011**, 13, 19378; b) T. Liu, Y. Ren, Y. Shen, S.-X. Zhao, Y. Lin, C.-W. Nan, *J. Power Sources* **2016**, 324, 349; c) A. Sharafi, H. M. Meyer, J. Nanda, J. Wolfenstine, J. Sakamoto, *J. Power Sources* **2016**, 302, 135; d) L. Cheng, E. J. Crumlin, W. Chen, R. Qiao, H. Hou, S. Franz Lux, V. Zorba, R. Russo, R. Kostecki, Z. Liu, K. Persson, W. Yang, J. Cabana, T. Richardson, G. Chen, M. Doeff, *Phys. Chem. Chem. Phys.* **2014**, 16, 18294; e) W. Luo, Y. Gong, Y. Zhu, K. K. Fu, J. Dai, S. D. Lacey, C. Wang, B. Liu, X. Han, Y. Mo, E. D. Wachsman, L. Hu, *J. Am. Chem. Soc.* **2016**, 138, 12258; f) K. Fu, Y. Gong, Z. Fu, H. Xie, Y. Yao, B. Liu, M. Carter, E. Wachsman, L. Hu, *Angew. Chem., Int. Ed.* **2017**, 56, 14942; g) C. Wang, Y. Gong, B. Liu, K. Fu, Y. Yao, E. Hitz, Y. Li, J. Dai, S. Xu, W. Luo, E. D. Wachsman, L. Hu, *Nano Lett.* **2017**, 17, 565; h) X. Han, Y. Gong, K. Fu, X. He, G. T. Hitz, J. Dai, A.

Pearse, B. Liu, H. Wang, G. Rubloff, Y. Mo, V. Thangadurai, E. D. Wachsman, L. Hu, *Nat. Mater.* **2016**, 16, 572; i) Y. Li, X. Chen, A. Dolocan, Z. Cui, S. Xin, L. Xue, H. Xu, K. Park, J. B. Goodenough, *J. Am. Chem. Soc.* **2018**, 140, 6448; j) Y. Shao, H. Wang, Z. Gong, D. Wang, B. Zheng, J. Zhu, Y. Lu, Y.-S. Hu, X. Guo, H. Li, X. Huang, Y. Yang, C.-W. Nan, L. Chen, *ACS Energy Lett.* **2018**, 3, 1212.

[9] a) N. J. Taylor, S. Stangeland-Molo, C. G. Haslam, A. Sharafi, T. Thompson, M. Wang, R. Garcia-Mendez, J. Sakamoto, *J. Power Sources* **2018**, 396, 314; b) Y. Song, L. Yang, W. Zhao, Z. Wang, Y. Zhao, Z. Wang, Q. Zhao, H. Liu, F. Pan, *Adv. Energy Mater.* **2019**, 9, 1900671; c) A. Sharafi, C. G. Haslam, R. D. Kerns, J. Wolfenstine, J. Sakamoto, *J. Mater. Chem. A* **2017**, 5, 21491; d) A. Sharafi, E. Kazyak, A. L. Davis, S. Yu, T. Thompson, D. J. Siegel, N. P. Dasgupta, J. Sakamoto, *Chem. Mater.* **2017**, 29, 7961; e) Y. Lu, X. Huang, Y. Ruan, Q. Wang, R. Kun, J. Yang, Z. Wen, *J. Mater. Chem. A* **2018**, 6, 18853; f) J. Duan, W. Wu, A. M. Nolan, T. Wang, J. Wen, C. Hu, Y. Mo, W. Luo, Y. Huang, *Adv. Mater.* **2019**, 31, 1807243; g) R. H. Basappa, T. Ito, H. Yamada, *J. Electrochem. Soc.* **2017**, 164, A666; h) Y. Suzuki, K. Kami, K. Watanabe, A. Watanabe, N. Saito, T. Ohnishi, K. Takada, R. Sudo, N. Imanishi, *Solid State Ionics* **2015**, 278, 172; i) G. T. Hitz, D. W. McOwen, L. Zhang, Z. Ma, Z. Fu, Y. Wen, Y. Gong, J. Dai, T. R. Hamann, L. Hu, E. D. Wachsman, *Mater. Today* **2019**, 22, 50; j) C.-L. Tsai, V. Roddatis, C. V. Chandran, Q. Ma, S. Uhlenbruck, M. Bram, P. Heitjans, O. Guillon, *ACS Appl. Mater. Interfaces* **2016**, 8, 10617.